

RESEARCH

Open Access



# An improved CRISPR and CRISPR interference (CRISPRi) toolkit for engineering the model methanogenic archaeon *Methanococcus maripaludis*

Qing Du<sup>1,3†</sup>, Yufei Wei<sup>1,4†</sup>, Liuyang Zhang<sup>1†</sup>, Derong Ren<sup>1,2</sup>, Jian Gao<sup>5</sup>, Xiuzhu Dong<sup>1,2</sup>, Liping Bai<sup>3\*</sup> and Jie Li<sup>1,2\*</sup>

## Abstract

**Background** The type II based CRISPR-Cas system remains restrictedly utilized in archaea, a featured domain of life that ranks parallelly with Bacteria and Eukaryotes. *Methanococcus maripaludis*, known for rapid growth and genetic tractability, serves as an exemplary model for studying archaeal biology and exploring CO<sub>2</sub>-based biotechnological applications. However, tools for controlled gene regulation remain deficient and CRISPR-Cas tools still need improved in this archaeon, limiting its application as an archaeal model cellular factory.

**Results** This study not only improved the CRISPR-Cas9 system for optimizing multiplex genome editing and CRISPR plasmid construction efficiencies but also pioneered an effective CRISPR interference (CRISPRi) system for controlled gene regulation in *M. maripaludis*. We developed two novel strategies for balanced expression of multiple sgRNAs, facilitating efficient multiplex genome editing. We also engineered a strain expressing Cas9 genomically, which simplified the CRISPR plasmid construction and facilitated more efficient genome modifications, including markerless and scarless gene knock-in. Importantly, we established a CRISPRi system using catalytic inactive dCas9, achieving up to 100-fold repression on target gene. Here, sgRNAs targeting near and downstream regions of the transcription start site and the 5' end ORF achieved the highest repression efficacy. Furthermore, we developed an inducible CRISPRi-dCas9 system based on TetR/*tetO* platform. This facilitated the inducible gene repression, especially for essential genes.

**Conclusions** Therefore, these advancements not only expand the toolkit for genetic manipulation but also bridge methodological gaps for controlled gene regulation, especially for essential genes, in *M. maripaludis*. The robust toolkit developed here paves the way for applying *M. maripaludis* as a vital model archaeal cell factory, facilitating fundamental biological studies and applied biotechnology development of archaea.

<sup>†</sup>Qing Du, Yufei Wei and Liuyang Zhang contributed equally to this work.

\*Correspondence:  
Liping Bai  
bailiping@caas.cn  
Jie Li  
lijie824@im.ac.cn

Full list of author information is available at the end of the article



© The Author(s) 2024. **Open Access** This article is licensed under a Creative Commons Attribution-NonCommercial-NoDerivatives 4.0 International License, which permits any non-commercial use, sharing, distribution and reproduction in any medium or format, as long as you give appropriate credit to the original author(s) and the source, provide a link to the Creative Commons licence, and indicate if you modified the licensed material. You do not have permission under this licence to share adapted material derived from this article or parts of it. The images or other third party material in this article are included in the article's Creative Commons licence, unless indicated otherwise in a credit line to the material. If material is not included in the article's Creative Commons licence and your intended use is not permitted by statutory regulation or exceeds the permitted use, you will need to obtain permission directly from the copyright holder. To view a copy of this licence, visit <http://creativecommons.org/licenses/by-nc-nd/4.0/>.

**Keywords** CRISPR toolbox, CRISPR interference, Multiplex genome editing, Gene expression, Archaea, Methanogen, *Methanococcus maripaludis*

## Background

Archaea represent the third domain of cellular life together with the domains of Bacteria and Eukarya. They are widely distributed on the Earth and play vital roles in the Earth's biogeochemical cycles [1–5]. Their dramatic and unique metabolic capabilities and extreme environment adaptabilities also confer them the potentials in biotechnological innovations and new applications [6–10]. However, despite their ubiquity and vital roles in Earth, our insights on archaeal biology and biotechnology are still largely lagged that of bacteria and eukaryotes, which are mostly attributed to their recalcitrant to be pure-cultured in lab and even harder to be genetically manipulated. To address these gaps, developing powerful genetic manipulation tools in representative and pure cultured archaeal species appears particularly important.

*Methanococcus maripaludis*, distinguished by its rapid growth, fully sequenced-genome, and genetically tractability, stands out as an archaeal representative species [11–14]. It is a methanogenic archaeon and utilizes CO<sub>2</sub>/H<sub>2</sub> or formate as its sole energy and carbon source for biomass and methane generation. The capability of converting CO<sub>2</sub> and H<sub>2</sub> into CH<sub>4</sub> and its fast autotrophic growth on CO<sub>2</sub> have facilitated *M. maripaludis* as an attractive archaeal chassis in inexpensively producing high-value biochemical products, such as hydrogen, methanol, geraniol and bioplastics [6, 10, 15], demonstrating the high potential of *M. maripaludis* as a superior CO<sub>2</sub>-fixing cell factory for fundamental and experimental biotechnology research. This species is also regarded as a model archaeon in archaeal biology research, such as in transcription and posttranscription regulation [16–20], motility characteristics [21, 22], featured CO<sub>2</sub> and N<sub>2</sub> fixation, and methanogenic metabolism [23–30]. Efficient and reliable genome-editing tools are critical for necessary genetic operation and modification in fundamental biological research and for successful metabolic engineering in biotechnology research. Therefore, to solve the limitations of the conventional genetic manipulation tools for *M. maripaludis*, such as the lack of enough resistance markers, laborious genetic selections for multiplex gene modifications, incapability of generating the markerless mutations with single nucleotide and multiple nucleotides, CRISPR-Cas9 and CRISPR-Cas12a system have been developed to achieve faster, more efficient, and more versatile genome editing in *M. maripaludis* [31, 32].

The CRISPR-Cas (clustered regularly interspaced short palindromic repeats and the associated *cas* genes) systems, known as the prokaryotic adaptive immune system to phages and foreign DNA elements, is commonly

present in bacteria and archaea [33–37]. In recent years, CRISPR-Cas systems have been developed as the best known key components of a new generation of genome editing tools [33–35]. The nuclease-deactivated Cas9 (dCas9), with H840A and D10A substitutions in the HNH and RuvC domains respectively, is inactivate at the endonuclease activity and only retains the sgRNA-guided DNA-binding ability [38]. Therefore, by selecting the sgRNA targeting sites, dCas9 can be directed by sgRNA to bind specific genomic loci and consequently can block the progress of RNA polymerase (RNAP) to the downstream genomic sequences and repress target gene expression. Thus, CRISPR interference (CRISPRi)-dCas9 have been developed as a powerful tool for fine-tuning transcription levels of a target gene, transiently or constitutively, and to be a preferable genetic engineering tool than other traditional genetic tools in bacteria [38–42]. However, CRISPRi-dCas9 is still limited to be developed in archaea and to our knowledge, it was only used to regulate gene expression in one archaeal species, *Methanosarcina acetivorans* [43].

To expedite the genetic manipulations in *M. maripaludis*, CRISPR-Cas system has been introduced and developed in this model archaeon [31, 32]. Utilizing a single editing plasmid containing a single guide RNA (sgRNA), Cas9, and a donor DNA sequence, the newly developed CRISPR-Cas9 tool has enabled precise and efficient genetic manipulations in *M. maripaludis* [31]. This includes efficient knockout of a single or double genes, large DNA fragments (~9 kb), and simultaneous editing of up to 13 genes across three genomic loci, and intricate in situ gene tagging and targeted nucleotide mutagenesis. Concurrently, the CRISPR-Cas12a tool was introduced into *M. maripaludis*, achieving up to 95% efficiency in deleting large genomic fragments, such as the ~9 kb segment encoding the flagellum operon [32]. Despite these improvements, the existing toolkits are limited to gene knockout and do not support gene regulation or knockdown. This limitation is particularly problematic for studying essential genes, where knockout could be lethal. Additionally, the CRISPR-Cas9 toolkit of *M. maripaludis* can still be improved for more efficient plasmid construction and multiplex gene editing [31]. Therefore, to address these issues, this study further refined the CRISPR-Cas9 tool in *M. maripaludis*, by developing strategies for streamlined construction of multiple sgRNAs, reducing CRISPR plasmid size by integrating Cas9 into the genome, and most importantly developing a CRISPR interference (CRISPRi) system for controlled gene regulation in *M. maripaludis*. These improvements

not only streamlined the multiplex genome editing and CRISPR plasmid construction but also introduced an inducible CRISPRi system to achieve controlled gene regulation, which is essential for advancing the study of essential gene functions. Therefore, these improvements have leveraged *M. maripaludis* as a model archaeal species for studying the archaeal fundamental biology and metabolic engineering for biotechnological applications.

## Results

### Improved sgRNA expression strategies for multiplex gene editing to achieve synchronous deletion of 13 genes in *M. maripaludis*

Previously, we developed a pMEV4-Cas9 editing system to achieve multiplex genome editing in *M. maripaludis* [31]. Through expressing four sgRNAs by four different promoter and terminator expressing cassettes in pMEV4-Cas9, we synchronously deleted 13 genes located at three different genomic loci. However, such approach would result in uneven editing efficiencies among the multiplex targeting genes by the different expression levels of sgRNAs and would also be application restricted by the limited defined promoters and terminators in *M. maripaludis*. Thus, to address these limitations, we implemented two novel genetic engineering strategies for multiplex genome editing in *M. maripaludis*. First, we standardized the expression of different sgRNAs by putting each of them under one same set of constitutive promoters (P0076) and terminators (T0204) (Fig. 1A), thus simplifying the construct and ensuring uniform sgRNA expression. After transforming the modified pMEV4-Cas9 plasmid with four sgRNAs targeting three different genomic loci, a ~9 kb large DNA fragment of the *fla* operon and two other distantly located genes (*aCPSF1b* and *aCPSF2*), we assayed the multiplex genome editing efficiency of such sgRNA expression strategy in *M. maripaludis*. Following selection via puromycin resistance, ten transformants were randomly selected for PCR assays, which use two sets of primer pairs to amplify the external and internal targeted editing regions of *aCPSF2*, *aCPSF1b*, and the *fla* operon, respectively. The PCR results clearly demonstrated that 100% editing efficiency was achieved across all targeted regions in all ten selected transformants (Fig. 1B). This evidence unequivocally indicates that utilizing a single set of promoters and terminators to express multiple sgRNAs and target multiple targets, represents an effective approach for conducting multiplex genome editing within *M. maripaludis*.

Second, we innovated another genetic engineering strategy for multiplex genome editing in *M. maripaludis* by co-transcribing four sgRNAs under a single promoter and terminator pair, but inserting a specific endoribonuclease sequence featured with a 10-nt motif of 'UNMND↓NUNAY' [20, 44] between sgRNAs for

their processing to generate separate sgRNA for multiplex genome editing (Fig. 2). The 10-nt motif sequence has been demonstrated to be efficiently cleaved by an endoribonuclease in *M. maripaludis* [20, 44], which provides a robust in vivo system for processing the co-transcribed sgRNAs for multiplex genome editing in *M. maripaludis*. Similarly, after transforming the modified pMEV4-Cas9 plasmid and selected by puromycin resistance, we assayed the multiplex genome editing efficiency by PCR amplification using two primer pairs to amplify the external and internal targeted editing regions of *aCPSF2*, *aCPSF1b*, and the *fla* operon, respectively. The results demonstrated a 100% editing efficiency for *fla* operon and near 100% editing efficiencies for *aCPSF2* and *aCPSF1b* in each of the 10 randomly selected transformants (Fig. 2). Successful deletion of *fla* operon was observed in all 10 transformants using primers to amplify both the external and internal editing regions (Fig. 2B, *fla* operon). Successful deletions of *aCPSF2* and *aCPSF1b* were observed in 8 of 10 selected transformants using primers to amplify the external editing regions of them, while faint PCR products were observed in two transformants (lanes 1 and 3 in Fig. 2B) using primers to amplify the internal editing regions. This suggests that the *fla* operon was completely edited in all 10 transformants and *aCPSF2* and *aCPSF1b* genes were also completely edited in 8 transformants (80%). Although *aCPSF2* and *aCPSF1b* genes were not completely edited in the other 2 transformants on all the ~55 chromosome copies [45], most (~90%) of the chromosome copies have been edited, based on the quantified band intensity of the PCR products (Fig. 2B lanes 1 and 3, right panel) compared to that of the control (Fig. 2B lane CK, right panel). Thus, this result clearly demonstrated that by co-transcribing multiple sgRNAs and then processed in vivo into individual, synchronous deletions of 13 genes were at least achieved in 80% transformants on all the ~55 chromosome copies of *M. maripaludis* through a single transformation step. This also implied that the co-transcribed sgRNAs could be processed at the implemented 10-nt motif sequence, referring to the intrinsic endoribonuclease activity in *M. maripaludis* [19], and thus an efficient multiplex genome editing could be obtained.

Consequently, these two novel sgRNA expression strategies circumvent the constraints of the available promoters and terminators to mitigate the possible uneven expression levels of different sgRNAs. Therefore, these strategies add to guarantee the versatility and efficiency of the multiplex genome editing within *M. maripaludis* and may also provide some reference for other archaeal or bacterial species for expressing multiple sgRNAs and achieve efficient multiplex genome editing.

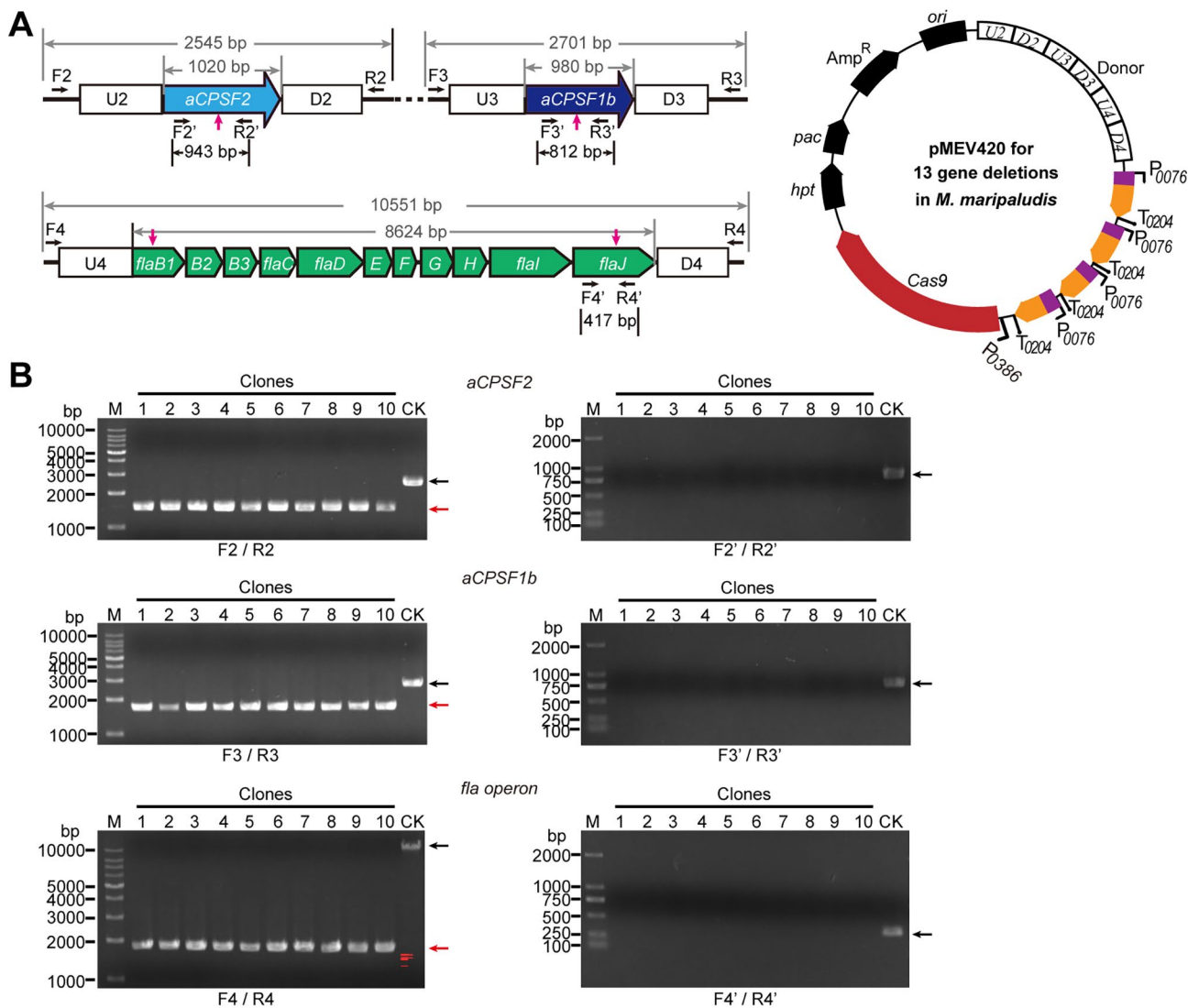


**Fig. 1** Improvement of CRISPR-Cas9 tool for multiplex genome editing by expressing multiple sgRNAs using one same set of promoters and terminators in *M. maripaludis*. **(A)** Schematic of the CRISPR-Cas9 plasmid (right, ~ 14 Kb) designed for the synchronous deletion of 13 genes located at three genomic loci (left) as shown. The 13 targeting genes include the whole *fla* operon genes (*MMP1666* to *MMP1676*), *aCPSF2* (*MMP0431*), and *aCPSF1b* (*MMP1381*). Four sgRNAs that target the coding regions (magenta arrows) of *aCPSF2*, *aCPSF1b*, *flaB1* (*MMP1666*), and *flaJ* (*MMP1676*) were expressed by each fused downstream of the promoter P0076 of *MMP0076* and terminator T0204 of *MMP0204*. The sizes of PCR amplification regions using indicated primers and the deleted genomic regions are shown. The homologous arms (~ 800 bp) of upstream (U2, U3, and U4) and downstream (D2, D3, and D4) sequences of each gene were concatenated on plasmid pMEV420 as the donor for homologous recombination repair. Cas9 was expressed under a strong promoter of P0386 in pMEV420. **(B)** PCR assays the successful knock-out of target genes in ten randomly selected puromycin-resistant transformants. Primer pairs of F2/R2, F3/R3, F4/R4, and F2'/R2', F3'/R3', F4'/R4' were used to amplify the external and internal regions of *aCPSF2*, *aCPSF1b*, and *fla* operon respectively as shown in (A). PCR products amplified from the wild-type (lane CK) and the mutated genomes (lanes 1–10) were indicated by black and red arrows, respectively. dsDNA marker (lane M) sizes were shown at left

### Establishing a genomic integrated Cas9 to improve the CRISPR editing performance

Given the large size of the Cas9 gene of 4.1 kb, the conventional pMEV4-Cas9 plasmids for genome editing in *M. maripaludis* usually exceed 11 kb, even to be > 15 kb when expressing four sgRNAs for multiplex genome editing described above, challenging both the plasmid construction efficiency in *E. coli* and subsequent transformation into *M. maripaludis*. Thus, to bypass these

challenges, we shorten the plasmid size by integrating the Cas9 gene into the genome. Via homologous recombination, the Cas9 expression cassette was inserted in the intergenic region between *MMP0852* and *MMP0853* (Figure S1A and S1B), one of the chromosomal neutral sites that were recently determined in *M. maripaludis* [46]. After selecting the positive transformants and PCR screening, we verified the correct integration of the Cas9 cassette in the targeted genomic locus by DNA

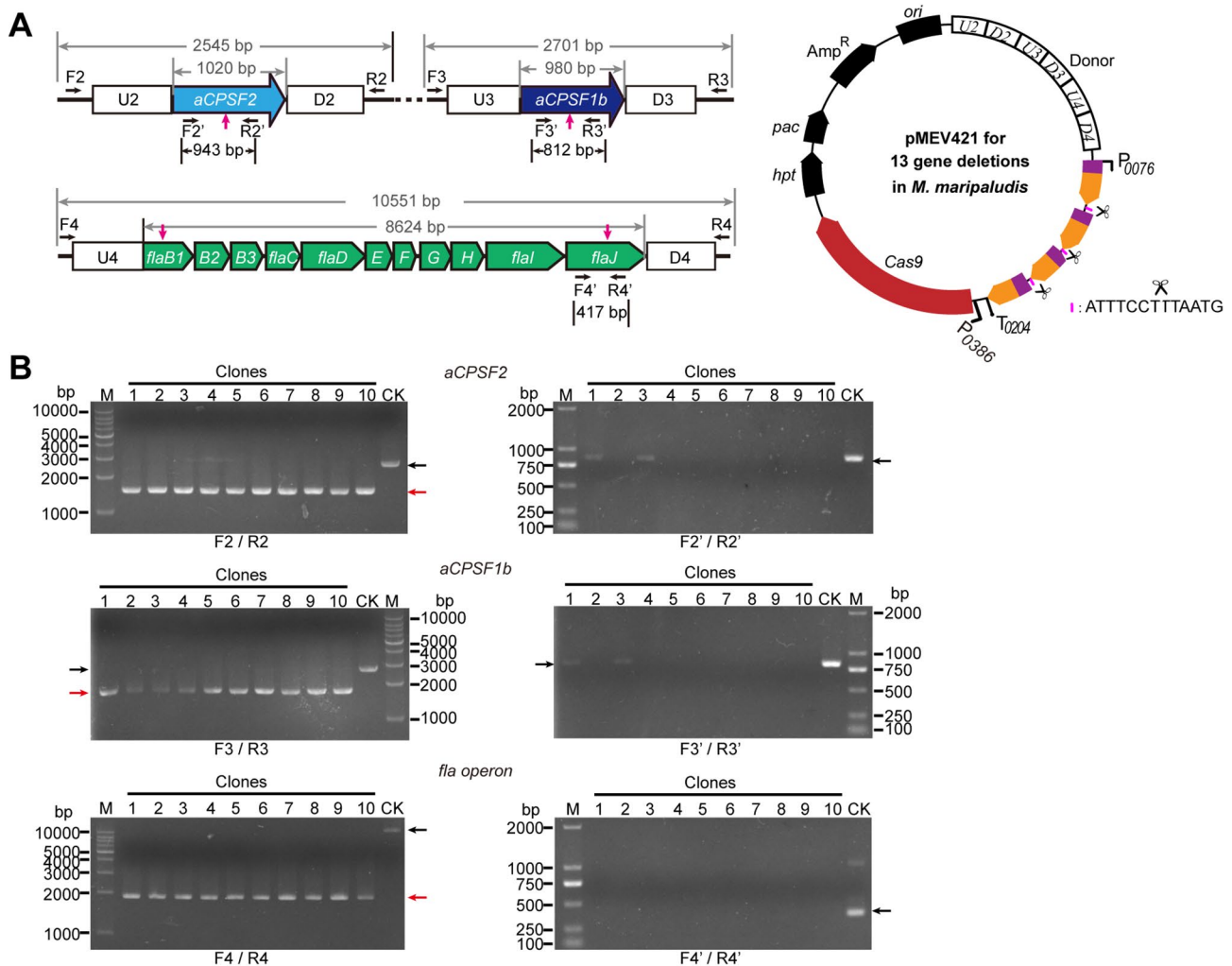


**Fig. 2** Improvement of the CRISPR-Cas9 tool for multiplex genome editing by expressing multiple sgRNAs via a co-transcription coupled with processing by a 10-nt endonuclease sequence in *M. maripaludis*. **(A)** Schematic of the CRISPR-Cas9 plasmid (right, ~14 Kb) designed for the synchronous deletion of 13 genes that are located at the three shown genomic loci (left). Four sgRNAs that target the coding regions (magenta arrows) of *aCPSF2*, *aCPSF1b*, *flaB1* (*MMP1666*), and *flaJ* (*MMP1676*) were co-transcribed by genetic cassette of P0076 and T0204, and processed by the intergenic 10-nt endonuclease sequence between them in *M. maripaludis*. The sizes of PCR amplification regions using indicated primers and the deleted genomic regions are shown. The homologous arms (~800 bp) of sequences upstream (U2, U3, and U4) and downstream (D2, D3, and D4) of each gene were concatenated on pMEV410 plasmid as the donor for homologous recombination repair. The Cas9 was expressed under a strong promoter of P0386 in pMEV410. **(B)** PCR assays the successful knock-out of target genes in ten randomly selected puromycin-resistant transformants. Primer pairs of F2/R2, F3/R3, F4/R4, and F2'/R2', F3'/R3', F4'/R4' were used to amplify the external and internal regions of *aCPSF2*, *aCPSF1b*, and *fla* operon respectively as shown in **(A)**. PCR products amplified from the wild-type (lane CK) and the mutated genomes (lanes 1–10) were indicated by black and red arrows, respectively. dsDNA marker (lane M) sizes were shown at left

sequencing. Then, using western blot, we detected a similar and slightly (~1.3-fold) higher expression level of Cas9 in the genome than that in the pMEV4-Cas9 plasmid (Figure S1C, quantified by Image J as indicated in the Figure legend). This demonstrated that Cas9 has been successfully expressed in the modified strain, hereby designated *M. maripaludis* S9. Additionally, we found that strain S9 exhibits a similar growth pattern as the parent *M. maripaludis* S0001 (Figure S1D). Therefore, the genome encoded Cas9 has been successfully expressed and exhibited no detectable toxicity to the host cells.

Next, we tested the genome editing efficacies of strain S9 by performing the deletion editing of two genes, large DNA fragment, and multiple genes, respectively. The CRISPR plasmids without Cas9 encoding cassette (Table S1, Fig. 3 and S2) were constructed much easier and more efficient, compared with the previous pMEV4-Cas9 plasmids. After transforming the Cas9-devoid CRISPR plasmids into the strain S9, 8–10 puromycin resistant transformants were randomly selected for PCR assays to evaluate the genome editing efficiency. Notably, 100% editing efficiency was observed in all the selected

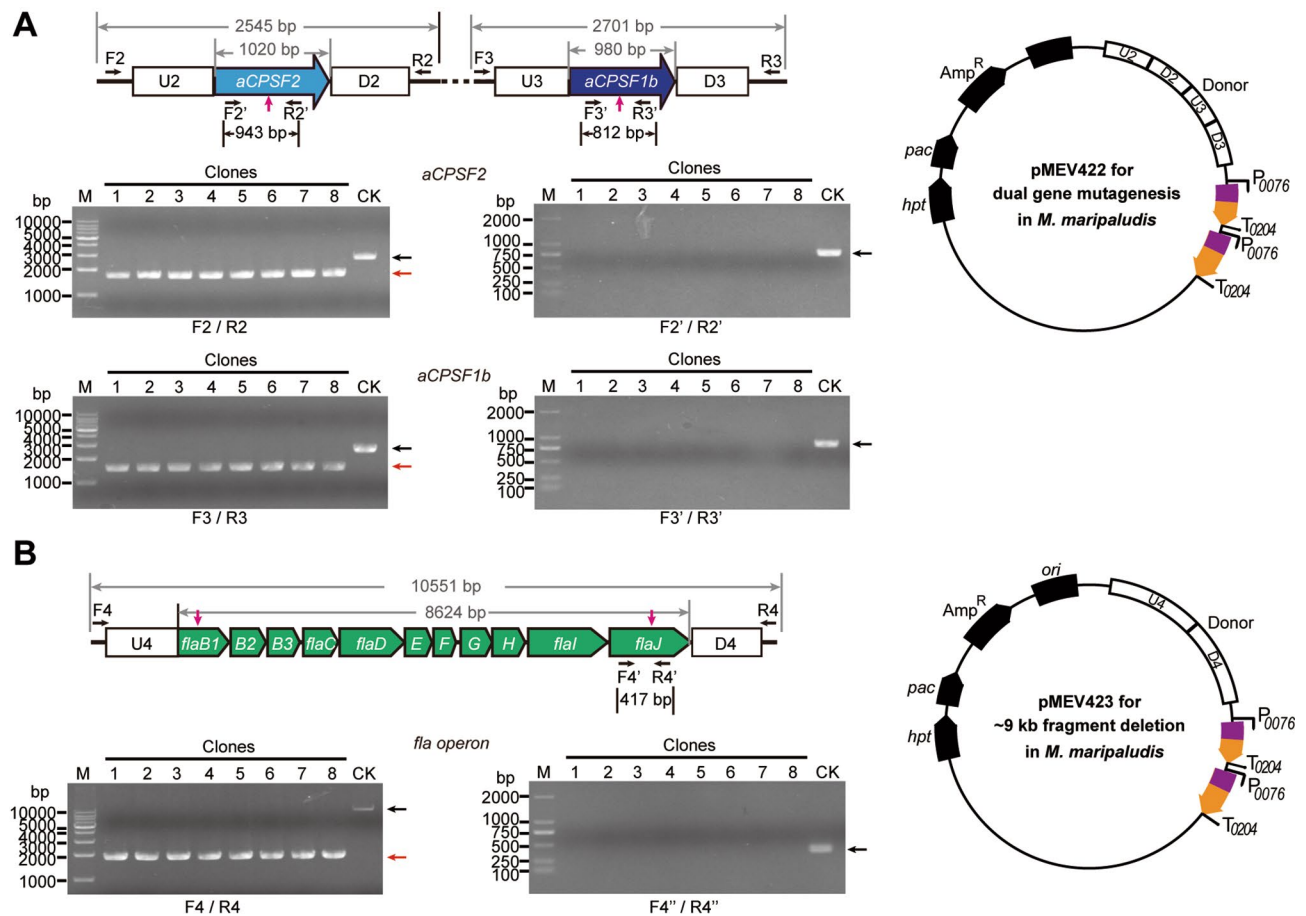


**Fig. 3** Synchronous deletion of two genes or a ~9 kb large DNA fragment assayed in *M. maripaludis* strain S9 that carries the Cas9 expression cassette in the genome. Schematic (top) shows the synchronous editing of the genes *aCPSF2* and *aCPSF1b* in (A) and the ~9 kb DNA fragment in (B). Plasmid pMEV422 (right) encodes two sgRNAs targeting the coding regions (magenta arrows) of the two genes, and the donors with sequences upstream (U2 and U3) and downstream (D2 and D3) of each target gene concatenated on pMEV422 for homologous recombination repair. Plasmid pMEV423 encodes two sgRNAs targeting the coding regions of the two genes (*flaB1* and *flaJ*) in the *fla* operon, and the donor with sequences upstream (U4) and downstream (D4) of target gene concatenated on pMEV423 for homologous recombination repair. The sizes of PCR amplification regions using indicated primers and the deleted genomic regions are shown. Eight randomly selected puromycin-resistant transformants subjected to PCR assay to determine the knock-out of target genes. Primer pairs of F2/R2, F3/R3, F4/R4, and F2'/R2', F3'/R3', F4'/R4' were used to amplify the external and internal regions of *aCPSF2*, *aCPSF1b*, and *fla* operon respectively as shown at the top panel. PCR products amplified from the wild-type (lane CK) and the mutated genomes (lanes 1–8) are indicated by black and red arrows, respectively. dsDNA marker (lane M) sizes are shown

transformants across the various tested genome editing, including double-gene deletion (Fig. 3A), large DNA fragment excision (Fig. 3B), and complex multiplex gene editing (Figure S2). In the parallel experiments of genome editing using the strain S9 or pMEV4-Cas9 system, it appeared that the strain S9 possesses a superior genome editing efficiency. This improvement is likely attributed to the slightly higher expression levels of Cas9 in the strain S9 compared to that in pMEV4-Cas9 system (Figure S1B). Therefore, the strain S9 emerges as a preferable option for CRISPR-based genomic modifications in *M. maripaludis*, offering enhanced precision and efficiency in genetic engineering applications.

### Development of one-step marker-less and scar-less gene knock-in editing in *M. maripaludis* S9

Marker-less and scar-less gene knock-in is pivotal for the expression of both endogenous and heterogeneous genes without introduction of accompanied marker genes and interfering the context genes. Consequently, we aimed to develop such genetic modification in *M. maripaludis* using strain S9. In strain S9 with knocking-out *aCPSF2* and *aCPSF1b* (Fig. 3A), we tested gene knock-in editing efficiency. The CRISPR plasmid for knocking-in *aCPSF2* and *aCPSF1b* was designated by expressing an sgRNA targeting the genomic region where *aCPSF2* was deleted, and the donor sequences for the inserted *aCPSF2* and *aCPSF1b* genes flanked by the *aCPSF2* upstream and downstream homologous arms (Fig. 4A).

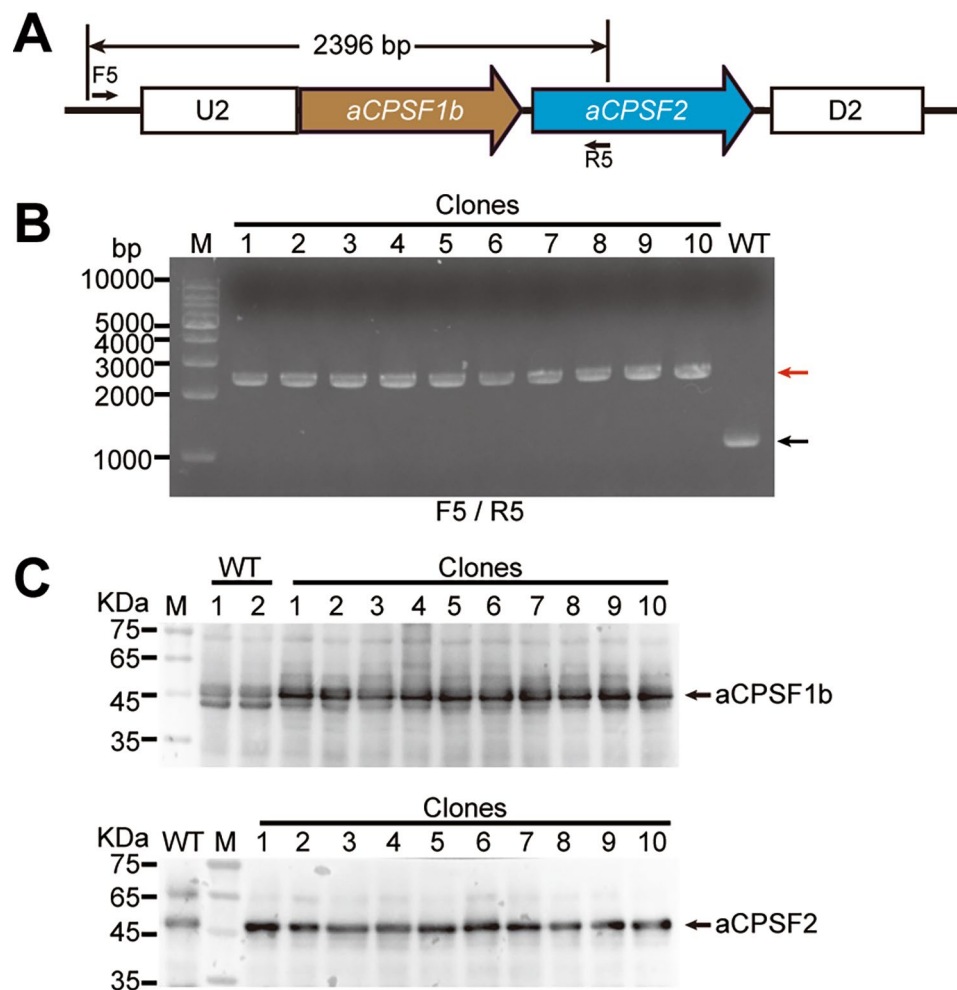


**Fig. 4** The marker-less and scar-less knock-in assay in *M. maripaludis* strain S9. **(A)** Schematic shows the DNA fragment carrying the *aCPSF2* and *aCPSF1b* expressing cassette that was knocked-in to the *M. maripaludis* strain S9 with *aCPSF2* and *aCPSF1b* being deleted, i.e., the mutated strain constructed in Fig. 3A. A sgRNA targeting the genomic region where *aCPSF2* was knockout and the donor with sequences upstream (U2) and downstream (D2) of *aCPSF2* and the cassette expressing *aCPSF2* and *aCPSF1b* inserted between U2 and D2 were cloned in the plasmid pMEV4-Cas9. **(B)** PCR assayed the knock-in of target genes in ten randomly selected puromycin-resistant transformants. Primer pairs of F5, targeting the genomic region upstream U2, and R5, targeting the coding region of *aCPSF2* (as illustrated at the top panel), were used to verify the insertion of the donor sequence into the genome. PCR products amplified from the wild-type (lane WT) genome carrying *aCPSF2* and *aCPSF1b* genes and the mutated genomes (lanes 1–10) carrying the knock-in fragment were indicated by black and red arrows, respectively. dsDNA marker (lane M) sizes were shown at left. **(C)** Western blot assayed the expression of *aCPSF1b* and *aCPSF2* in selected positive knock-in transformants in **(B)** and the wild-type strain (lane WT) using the anti-*aCPSF1b* and anti-*aCPSF2* antibodies. Cell-free extract of the wild-type (WT) strain S9 of *M. maripaludis* was used as reference

After transforming the modified CRISPR plasmid and selecting for puromycin resistance colonies, PCR screening, followed by DNA sequencing confirmed the correct insertion of *aCPSF2* and *aCPSF1b* genes at the targeted locus in all the 10 selected transformants (Fig. 4B). Western blot assay further validated the successful expression of *aCPSF2* and *aCPSF1b* proteins in all the 10 selected transformants (Fig. 4C).

#### Utilizing CRISPRi-dCas9 to modulate gene expression in *M. maripaludis*

Next, we innovatively adapted the CRISPR-Cas9 system into a CRISPR interference (CRISPRi) system for

achieving controlled gene expression in *M. maripaludis*, which is still a challenging theme via both the conventional genetic tools and the developed CRISPR-Cas tools. By introducing targeted mutations at the Cas9 active sites, specifically D10A and H840A within the RuvC1 and HNH nuclease domains, respectively, we generated a nuclease-deactivated Cas9 (dCas9) [38]. This modified enzyme was incorporated into the pMEV4 CRISPR plasmid, subsequently renamed as pMEV4-dCas9, tailored for gene repression studies in *M. maripaludis* (Table S1). To systematically evaluate the regulatory effects of the constructed pMEV4-dCas9 system in *M. maripaludis*, two non-essential genes, those were

determined previously [47], *MMP1718* and *MMP0372*, alongside with a heterologous *mCherry* cassette integrated at the intergenic region between *MMP0852* and *MMP0853*, were selected for testing. *MMP1718* encodes EarA, a pivotal regulator of the euryarchaeal archaellum [21, 22], and *MMP0372* encoding F420-dependent methylenetetrahydromethanopterin dehydrogenase, Mtd.

For each targeted gene, diverse sgRNAs targeting different regions (Table S3) were designed to direct dCas9-mediated transcription repression to achieve controlled regulation of targeted gene. Specifically, five sgRNAs targeted *MMP0372* (*mtd*), eight sgRNAs targeted *mCherry*, and two sgRNAs targeted *MMP1718* (*earA*) (Fig. 5). After transforming pMEV4-dCas9 with one of the various sgRNAs into *M. maripaludis* S0001 and selecting for puromycin-resistant transformants, gene expression levels were quantified by RT-qPCR. The repression effects were assessed by comparing the target gene expression in these transformants carrying a gene targeting sgRNA to those harboring a control plasmid of pMEV4-dCas9 without sgRNA. Then, it was determined that substantial transcription repression of 93–99% (equivalent to

14.3–100-fold reduction) was observed in *MMP0372* (*mtd*) in transformants harboring pMEV4-dCas9 with either sgRNA2, 3, or 5. In contrast, only moderate repression ranging from 54 to 64% (approximately 2.1 to 2.7-fold reduction) was achieved with sgRNA1 and sgRNA4 (Fig. 5A).

Similarly, in the *mCherry* assays, substantial transcription repression of 89–94% (equivalent to ~9.1- to 16.7-fold reduction) was achieved with sgRNAs 2, 3, 5 to 8 targeting *mCherry*, while only slighter significant repression of 77–84% (equivalent to ~4.35- to 6.25-fold reduction) was observed with sgRNAs 1 and 4 targeting the promoter region of *mCherry* (Fig. 5B). In the assays of *MMP1718* (*earA*), the employment of pMEV4-dCas9 with two sgRNAs targeting downstream and near the transcription start site (TSS), resulted in significant transcription repression of 91–97% (11.1- to 33.3-fold reduction) on *MMP1718* (*earA*). Considering EarA's role as a transcription activator of the *fla* operon [21, 22], which encodes the archaellum's protein components, the transcription level of *MMP1666* (*flaB1*) and *MMP1670* (*flaD*) in the *fla* operon, were also quantified. It was determined

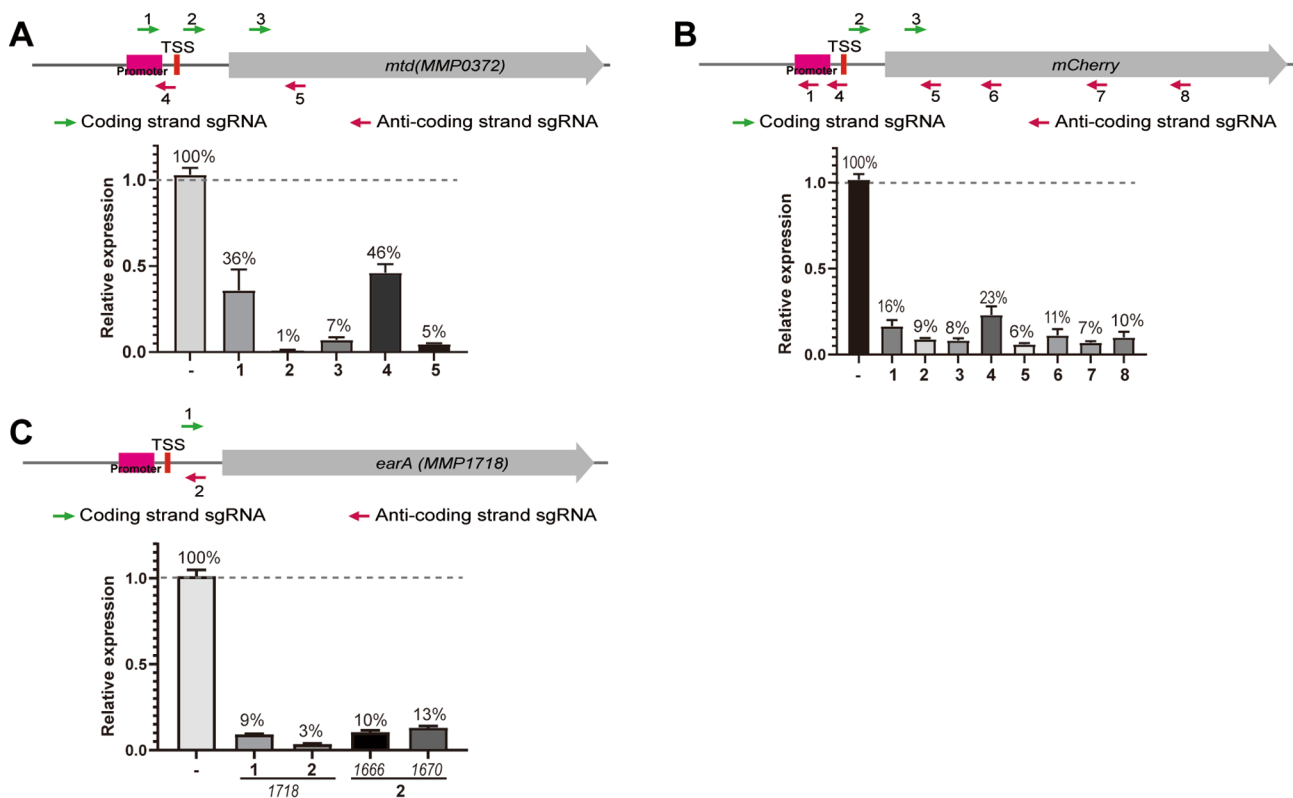


**Fig. 5** The CRISPRi-dCas9 based transcription repressions of target genes in *M. maripaludis*. Schematics at top show the sgRNAs targeting regions, such as promoters, transcription start site (TSS) proximal, coding strand and template strand. RT-qPCR quantified relative transcription abundances of *mtd* (*MMP0372*) (A), *mCherry* (B), and *earA* (*MMP1718*) (C) in CRISPRi-dCas9 strains with corresponding sgRNAs, one strain with each indicated sgRNA, were compared with that of the control strain (-) carrying with the plasmid of pMEV4-dCas9 without sgRNA. The *earA* regulated genes (*MMP1666* and *MMP1670*, *flaB1* and *flaD*) were also quantified in the *earA* knock-down strains based on CRISPRi-dCas9 system in (C). Bars represent the means from three biological replicates

that these two genes were significantly reduced as well (Fig. 5C), verifying the effective repression of EarA by this sgRNA guided dCas9 system.

These results conclusively demonstrate that sgRNAs targeting sequences downstream near TSS, as well as the 5' end of ORF region, effectively guide dCas9 to achieve significant repression, often exceeding or approaching 10-fold reductions. Therefore, for optimal gene repression using CRISPRi-dCas9 in *M. maripaludis*, it is advisable to select sgRNAs targeting areas proximal to and downstream of the TSSs, as well as along with the 5' end regions of the ORFs of target genes.

#### Development of an inducible CRISPRi-dCas9 system for controllable gene repression on essential genes in *M. maripaludis*

The lack of genetic tools to manipulate essential genes in *M. maripaludis* has hindered its utility as a model species for elucidating the role of conserved essential genes in crucial biological processes of archaea. To address this, we motivated to develop an inducible CRISPRi-dCas9 system for controllable gene repression in *M. maripaludis*.

Initially, we selected a tetracycline-inducible TetR/*tetO* genetic cassette, previously used to regulate expression of the archaeal general transcription termination factor, aCPSF1, in *M. maripaludis* [16]. We incorporated this cassette into two potent promoters, P0386 and P0667, recently characterized in *M. maripaludis* [46], to screen for superior inducible promoters for dCas9 expression. Synthetic promoters were constructed by fusing one or two *tetO* sequences up- or downstream the TSSs of the two promoters, resulting in six synthetic promoters for evaluating the tetracycline inducible expression of the fused reporter gene of *mCherry* (Fig. 6A and S3A). We chose anhydrotetracycline (aTc), a tetracycline analog known for its minimal toxicity and strong TetR binding in bacteria, for our assays. The TetR expression cassette and the *tetO*-P0386/P0667-*mCherry* cassette were cloned into pMEV4 plasmids and transformed into *M. maripaludis*. In the absence of aTc, the P0383-*tetO2*, with two *tetO* sequences, exhibited minimal fluorescence, less than 1% compared to the wild-type P0383, indicating effective repression by TetR. Similar but slightly less repression was observed for P0383-*tetO1* and P0383-*tetO3* promoters, which have single *tetO* sequence fused up- and downstream TSS respectively. Upon addition of aTc, significant increase in fluorescence were observed across all P0383-derived promoters (Fig. 6B), demonstrating aTc-mediated depression by TetR disassociation from *tetO*. The most substantial upregulation was recorded for P0383-*tetO3* after 4 h post-addition of aTc, approaching wild-type level of P0383 (Fig. 6B). At 2  $\mu\text{g/ml}$  aTc, the aTc inducible expression increased by 4.5-fold for P0383-*tetO1*, 17-fold

for P0383-*tetO2*, and 6-fold P0383-*tetO3* respectively. Similar patterns were observed across aTc concentrations of 5–20  $\mu\text{g/ml}$  (Fig. 6B). Studies on the impact of aTc on growth revealed negligible effects at  $\leq 2$   $\mu\text{g/ml}$ , while higher concentrations ( $\geq 20$   $\mu\text{g/ml}$ ) inhibited the growth significantly (Figure S4). These results underscore the robust regulatory capacity of TetR/*tetO* system on P0383-*tetO* promoters. Similar TetR/*tetO* regulation could be observed on three synthetic P0667-*tetO* promoters as well, albeit with lower inducibility compared to P0383 variants (Figure S3B). Therefore, we chose P0383-derived promoters for further exploring the possible applications in obtaining the inducible CRISPRi-dCas9 in *M. maripaludis*.

We then selected the P0383-*tetO3* promoter to evaluate the aTc induction on dCas9 expression. Western blot assay demonstrated a minimal dCas9 abundance without aTc, while its abundance notably increased after aTc was added, indicating the efficacy of the TetR/P0383-*tetO3* system in modulating dCas9 expression through adjusting the absence or presence of aTc. Subsequently, we investigated if this inducible expression of dCas9 could achieve the inducible gene repression on targeting genes. Using sgRNAs that previously demonstrated effective repression of *MMP0372* (*mtd*) and *MMP1718* (*earA*) (Fig. 5A and C), we explored the inducible gene repression using the TetR-*tetO* coupled CRISPRi-dCas9 system. Compared to the control, *MMP0372* expression in the strain harboring TetR-*tetO* coupled CRISPRi-dCas9 and sgRNA1 targeting the TSS of *mtd* decrease to 7% in the presence of aTc, from 64% in the absence of aTc (Fig. 6D). For *MMP1718* (*earA*), expression dropped to 15% from 88% with aTc induction (Fig. 6D). Therefore, these results demonstrated that the TetR/*tetO* system can effectively induce dCas9 expression, facilitating effective aTc induced repression on target genes tested here.

Furthermore, we explored the potential of this inducible CRISPRi-dCas9 system to knock down essential genes in *M. maripaludis*, specifically targeting *MMP0374*, which encodes Nob1, an essential endoribonuclease in the ribosomal RNA maturation process [47–49]. By designing a sgRNA targeting the sequence near and downstream the TSS of *MMP0374*, we tested the inducible repression on this gene using the TetR/*tetO* controlled dCas9. Compared to the control strain carrying the sgRNA-devoid CRISPRi-dCas9 plasmid, the expressions of *MMP0374* in the strain carrying the sgRNA and the TetR/*tetO* controlled CRISPRi-dCas9 system was quantified to be 73% in the absence of aTc, while it was determined to be only 2% when adding aTc to induce the expression of dCas9. Thus, this robust repression demonstrates that the inducible CRISPRi-dCas9 system constructed here provides a potent approach for the

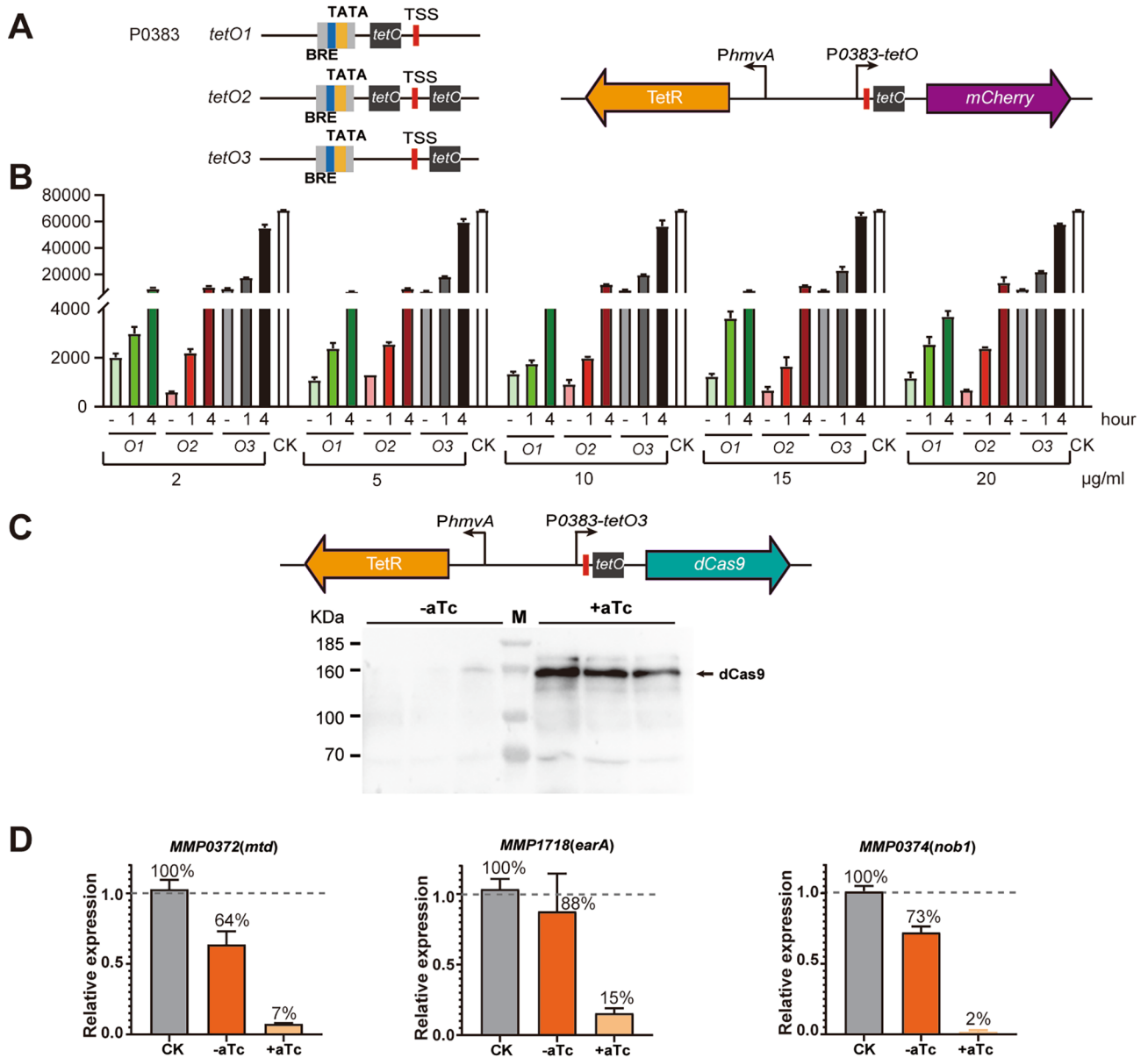


**Fig. 6** Controlled gene repressions using the inducible CRISPRi-dCas9 system developed in *M. maripaludis*. **(A)** Schematic shows three versions of TetR/*tetO* inducible promoters, fusing *tetO* sequences adjacent to the P0383 as shown (left), and then each was fused with the mCherry reporter gene, while TetR was under the control of *PhmvA* (right). The inducibility of the designed TetR/*tetO* promoters was assayed by mCherry fluorescence in *M. maripaludis*. **(B)** Fluorescence intensities of mCherry were assayed at three *tetO* fused P0383 promoters (P0383-*tetO1*, P0383-*tetO2*, and P0383-*tetO3* were briefed as O1, O2, and O3, respectively). aTc of 2, 5, 10, 15, 20 μg/ml was added into the medium at the logarithmic phase respectively and the fluorescence was determined after 1–4 h induction. Fluorescence intensities of mCherry when expressed under the wild-type P0383 were used as the control (CK). Fluorescence intensities of mCherry were assayed in triplicate cultures, and averages and standard deviations are shown. **(C)** Schematic (top) shows the dCas9 was expressed using the anhydrotetracycline (aTc) inducible TetR/*tetO* system designed in this study. Western blot assayed the expression intensities of dCas9 in the TetR/*tetO* driven dCas9 in the absence or presence of aTc using the commercial anti-Cas9 antibody. **(D)** RT-qPCR quantified relative transcription abundances of *mtd* (MMP0372), *earA* (MMP1718) and *nob1* (MMP374) controlled by the inducible CRISPRi-dCas9 strains in the absence and presence of aTc. Transcription abundances of each gene in the control strain carrying sgRNA-devoid pMEV4-dCas9 were set as 100%. Data are the means from three biological replicates

controllable repression of essential genes, addressing a significant methodological gap in studying essential gene functions in this model archaeon.

#### **Mutation of *earA* by CRISPR-Cas9 and CRISPRi-dCas9 systems caused the archaellum and swimming phenotype changes in *M. maripaludis***

Given that *MMP1718* (*earA*) is the transcription activator of the *fla* operon encoding key components of archaeella in *M. maripaludis* [21, 22], the swimming organelle of archaea, we investigated the phenotype changes in the mobility of the *earA* mutated strains constructed in this study to assess the phenotype impacts of the CRISPR-based genomic modifications obtained here. The following strains were evaluated: the multiplex gene deletion strain of  $\Delta aCPSF2\Delta aCPSF1b\Delta fla$  constructed using pMEV4 plasmid (Fig. 1), the *fla* operon deletion strain by the genomic expressed Cas9 (Fig. 3B), the *earA* knock-down strain via CRISPRi-dCas9 (Fig. 5C), the *earA* knock-down strain using the inducible CRISPRi-dCas9 system (Fig. 6D), and the wild-type strain of *M. maripaludis* as a control. Through assaying the mobility phenotypes of these strains on soft agar plates, it was evident that compared to the wild-type, mutated strains with *earA* knock-out, knock-down, and inducible knock-down all generated noticeably smaller colony lawn sizes spread on the plates (Figure S5), demonstrating reduced mobility abilities. Therefore, this result confirmed that modifying the *earA* gene expression via CRISPR-Cas9 or CRISPRi-dCas9 systems all resulted in discernible changes in physiological phenotypes.

#### **Discussion**

To date, the development of CRISPR-Cas tools in archaea lags significantly behind their counterparts in eukaryotes and bacteria. This limitation has impeded progress in both basic and applied research within the field of archaeal biology and biotechnology. This study presents several advancements in the CRISPR-Cas9 toolkit for *M. maripaludis*, including novel sgRNA expression strategies, integration of Cas9 into the genome, and the development of both a CRISPR interference (CRISPRi) system and a tetracycline-regulated CRISPRi-dCas9 system. These innovations not only streamline multiplex genome editing and CRISPR plasmid construction but also introduce a controlled gene regulation system through inducible CRISPRi and facilitate controlled repression of essential genes. These enhancements have marked a leap over previous genetic manipulation capabilities and bridged a significant methodological gap for controlled gene regulations, especially for essential genes, in this representative archaeon. This meets the critical need to utilize *M. maripaludis* as a model archaeon for fundamental biological studies and biotechnological

applications, particularly as a microbial cell factory for producing biocatalysts and biochemicals.

CRISPR-Cas tools have revolutionized the capability in simultaneously manipulating multiple genes in a single genetic entity, which is of great value in both basic research and practical biotechnology applications dependent on genetic engineering. Recently, combination of the *Streptococcus pyogenes* Cas9 with proper transcribed sgRNAs, has been determined to be an efficient tool of generating gene knock-out, modifications and also multiplex genome editing in *M. maripaludis* [31]. However, the targeting capability and editing efficiency of this CRISPR-Cas9 tool were largely constrained by the sgRNA-expressing device and the Cas plasmid construction efficiency. Therefore, in this study, we improved these aspects for improving the editing efficiency of CRISPR-Cas9 system in *M. maripaludis*. By relocating the Cas9 cassette from the pMEV4-Cas9 plasmid to a neutral site in the genome (Figure S1A), we facilitated more efficient CRISPR-Cas plasmid construction and achieved superior genome editing outcomes (Fig. 3 and S2). Moreover, we introduced two novel strategies for expressing multiple sgRNAs: one utilizing a single set of promoter and terminator (P0076 and T0240) cassette for expressing different sgRNAs (Fig. 1), and another where multiple sgRNAs are co-transcribed but separated by a 10-nt endoribonuclease cleavage sequence for their processing (Fig. 2). Based on these strategies, multiplex genome editing for deleting 13 genes has achieved with 80-100% editing efficiency on all the ~55 chromosomal copies in *M. maripaludis*. Compared to the previous method of expressing multiple sgRNAs using different cassettes of promoters and terminators in multiplex genome editing, the new methods have some obvious advantages, such as but not limited to the available numbers of promoters and terminators, and that more even expression of different sgRNAs could facilitate equivalent genome editing efficiencies among different target genes. The 10-nt endoribonuclease cleavage sequence has been reported to be widely distributed with function important in mRNA and rRNA processing in methanogen *M. maripaludis* and *Methanolobus psychrophilus*, but can also be found in many archaeal species [20, 44], suggesting that such a strategy of expressing multiple sgRNAs as designed in this study could also be applicable to other archaeal species for multiplex genome editing. The endogenous tRNA-processing system was also used for processing multiple sgRNAs from a co-transcribed polycistronic RNA for multiplex genome editing in plants and halobacteria using a t-elements fold into tRNA-like structures [50, 51]. While compared with the tRNA elements, the 10-nt endoribonuclease cleavage sequence used here is 13-nt, which is much shorter than the tRNA elements used in plants and halobacteria and

could be more easily designed into the multiple sgRNA expressing device.

Thus far, the availability of genetic tools for the tunable control of gene expression in *M. maripaludis* remains limited, which has hindered its application as a microbial cell factory for metabolic engineering, and for investigating the functions of essential genes that are pivotal to understand archaea biology. Although a few inducible promoters for transcription control have been reported including a phosphate concentration regulated *pst* promoter and a TetR regulated *tetO* fused *nif* promoter [16, 52], the 4- to 6-fold regulation on target gene and a growth medium with phosphate concentration changes for the *pst* promoter may limit the utilization of these promoters. Therefore, more powerful tools for tunable regulation control of target genes in *M. maripaludis* are urgently required. This study not only introduce the CRISPRi-dCas9 system into *M. maripaludis* for achieving a up to 100-fold repression on targeted genes, but also designed six tetracycline regulated *tetO* fused archaeal promoters that can achieve a up to 17-fold induction on targeted gene expression (Figs. 5 and 6). Importantly, the TetR/*tetO* fused promoters designed in this study further facilitated the construction of the inducible CRISPRi-dCas9 system and achieved the tetracycline induced repression of essential genes in *M. maripaludis* (Fig. 6). Therefore, these molecular tools not only fill the methodological gap in studying essential gene functions but also broaden the potential for controllable genetic manipulations, enhancing the utility of this organism in synthetic biology and biotechnology applications. This represents the second implementation of CRISPRi-dCas9 system [43] and the first inducible CRISPRi-dCas9 system developed in archaea. Thus, the designed tetracycline regulated *tetO* promoters for inducible CRISPRi system may evidently have provided an obvious advantage than the known CRISPRi system in archaeal organisms [43], and the design approach for such system here could offer a reference for similar adaptations in other archaeal species.

To achieve high repression efficiency, it is an important prerequisite to select the appropriate regions of target gene for sgRNA targeting. By screening the sgRNA targeting sites on selected targets in *M. maripaludis*, sgRNAs targeting near the TSS near and close to the 5' end of the targeted ORF achieved the high repression efficiency (up to 99%). Additionally, the two new strategies of co-expressing multiple sgRNAs designed in this study could also be utilized in CRISPRi-dCas9 system to manipulate knocking-down multiple genes simultaneously, which is usually required in the simultaneous regulation of multiple genes in metabolic pathways in the synthetic biology studies. However, achieving high repression efficiency for a new target gene often requires

designing and testing multiple sgRNAs that target different regions, particularly those near TSS and close to the 5' ORF end. The efficiency of CRISPRi must be experimentally validated for each sgRNA. Additionally, the selection of sgRNA targeting sites is constrained by the presence of the NGG protospacer adjacent motif (PAM) sequence at the target gene. Consequently, it may be challenging to find suitable sgRNAs for certain genes, limiting the potential for achieving required gene repression efficiency. These factors may bring some restrictions on the effectiveness of the CRISPRi system in *M. maripaludis*.

Appropriate sgRNA targeting sites for achieving high repression on target genes are also required in other organisms. In a model halobacteria *Haloferax volcanii*, based on its endogenous type IB CRISPRi system, crRNAs targeting the promoter and the TSS regions of the template strand reduced transcript levels down to 8%, while crRNAs targeting the coding strand repress expression only down to 88% and the repression of an essential gene is only down to 22% [51, 53]. In the CRISPRi-dCas9 system of *M. acetivorans*, sgRNA targeting the promoter and the ORF regions of targeted genes, whatever in mono- or poly-cistron, achieved >85–90% reduction on targeted genes [43]. In *E. coli*, sgRNAs targeting the coding strand and the promoter region demonstrated efficient gene repression (10- to 300-fold), whereas those targeting the template strand exhibited slight effect [38]. In *Mycobacterium tuberculosis*, sgRNA targeting promoter and the 5' ORF region on coding strand determined efficient (>80%) gene repression, as well [39]. Therefore, to achieve a high repression efficiency based on CRISPRi systems, appropriate sgRNA targeting regions are needed to be chosen in both bacterial and archaeal organisms. It would be a good choice of co-express two sgRNAs, with one targeting the TSS proximal sequence and the other one targeting the coding region 5' end to achieve high repression on targeted gene in *M. maripaludis*.

In conclusion, this study developed enhanced CRISPR-Cas9 tool and CRISPRi-dCas9 toolkits that enable effective multiplex gene editing and tunable gene regulation in *M. maripaludis*. Consequently, these robust toolkits pave the way for advancing the use of this model archaeon in the studies of the fundamental archaeal biology and the biotechnological applications, particularly those based on CO<sub>2</sub> utilization.

## Materials and methods

### Strains, plasmids, and culture conditions

Plasmids and strains utilized in this study are listed in Table S1. Both parental and mutated strains of *M. maripaludis* were routinely cultured anaerobically in pre-reduced McF medium under a gas phase of N<sub>2</sub>/CO<sub>2</sub>

(80:20) at 37 °C, following previously described procedure [13]. Colonies were screened using a solid plating via supplementing 1.5% agar into the liquid medium. Puromycin (2.5 µg/mL) was used as marker gene for selection unless indicated otherwise, and the base analog 8-azahypoxanthine at 20 µg/mL was used for a counterselection for curing the Cas9-based pMEV4 plasmid as described previously [31, 54]. For the construction of plasmids and other fragments, *E. coli* DH5α or BL21(DE3)/pLysS was grown at 37 °C in Luria-Bertani (LB) broth or LB-agar plates, supplemented with ampicillin (100 µg/mL) when necessary. Growth was monitored by determining the optical density at 600 nm (OD600) with a spectrophotometer.

### Two new strategies of expressing multiple sgRNAs in pMEV4-Cas9 plasmids for multiplex genome editing in *M. maripaludis*

Plasmids used or constructed in this study are listed in Table S1, and the primers utilized for plasmid engineering and transformants screening are listed in Table S2. PCR amplification was performed using the high-fidelity KOD-plus DNA polymerase (TOYOBO, Japan). DNA fragments and the amplified plasmid backbone were ligated using the stepwise Gibson assembly using the ClonExpress MultiS one-step cloning kit (Vazyme).

pMEV4-Cas9 plasmids were constructed similarly as previously described [31], with the *Streptococcus pyogenes* Cas9 (SpCas9) [55] being codon optimized and expressed downstream a strong promoter of P0386 [31, 46]. The sgRNAs were expressed downstream promoters as indicated in Figs. 1, 2 and 3 and S2, and the donor DNA required for homologous recombination repair was inserted upstream the sgRNA cassette on the plasmid. Two new strategies for expressing multiple sgRNAs (Table S3) were performed to achieve efficient multiplex gene editing in *M. maripaludis* in this study. First, four sgRNAs targeting the coding regions of *aCPSF2*, *aCPSF1b*, and the *fla* operon (*flaB1* and *flaJ*) were expressed by one same set of promoter P0076 and Terminator T0204 (Table S3 and Fig. 1), whose activities have been assayed previously [17, 46]. Second strategy, the four sgRNAs were co-transcribed by one set of promoter P0076 and terminator T0204, and processed through a specific endoribonucleolytic sequence of a featured 10-nt motif of 'UNMND↓NUNAY' inserted between two sgRNA sequences (Table S3 and Fig. 2). The DNA sequences encoding the two different expression elements carrying multiple sgRNAs were synthesized in Co. Genscript (Suzhou, China) and inserted to the pMEV4-Cas9 plasmids. The donor DNA sequences were amplified from the genomic DNA and fused upstream the sgRNA cassette in pMEV4-Cas9 plasmids via the stepwise Gibson assembly kit. The constructed plasmids were

validated by DNA sequencing prior to being transformed into *M. maripaludis* S0001.

### Construction of the *M. maripaludis* strain S9 and the CRISPR plasmids for genome editing in S9

To shorten the CRISPR plasmid length for a more efficient construction efficiency, the Cas9 expression cassette (4.3 kb) was removed from the plasmid pMEV4-Cas9 to the genome (Figure S1A). The previously identified neutral site at the intergenic region (the genomic sites of 863885 and 863938 bp) between *MMP0852* and *MMP0853* of *M. maripaludis* S2 [17, 46] was chosen. The Cas9 expression cassette (4.3 kb) was amplified from the plasmid pMEV4-Cas9 and fused with the DNA fragments amplified from upstream of *MMP0852* and downstream of *MMP0853* from the genomic DNA for homologous recombination. The neomycin resistance gene cassette was amplified from the pMEV4 plasmid and inserted upstream the Cas9 expression cassette. The obtained DNA fragment was transformed into *M. maripaludis* S0001, a strain derived from *M. maripaludis* S2 [15, 56], via the PEG-mediated transformation procedure [13, 57]. Transformants were resistant to neomycin and verified by PCR amplification for the presence of the genomic Cas9 sequence and by assaying the expression of Cas9 via western blot assay. The obtained positive transformants that successfully express Cas9 on genome were designated as *M. maripaludis* S9.

The CRISPR plasmids for genome editing in *M. maripaludis* S9 for knock out of two genes (*aCPSF2* and *aCPSF1b*) and a ~9 kb DNA fragment encoding the *fla* operon, multiplex genome editing for 13 genes located at three genomic loci, as shown in Fig. 3 and S2, were constructed following a similar procedure as previously described [31] but without the large fragment that encodes Cas9. The obtained CRISPR plasmids were transformed into *M. maripaludis* S9 via the PEG-mediated transformation procedure and cured puromycin resistance transformants were obtained and verified.

### Construction of CRISPRi-dCas9 plasmids for knocking down target genes in *M. maripaludis*

To construct the CRISPRi-dCas9 gene repression system, the catalytically inactive dCas9 was obtained by mutating the Cas9 sequence of the pMEV4-Cas9 plasmid at the active sites of Cas9 (D10A and H840A in the RuvC1 and HNH nuclease domains respectively) using a site-directed mutagenesis kit (Stratagene) using the primers carrying mutagenesis sites listed in Table S2. Then, pMEV4-dCas9 plasmid was obtained. Promoter, TSS proximal, and the coding regions were chosen as targets for the sgRNA and repression efficiencies were assayed by RT-qPCR as shown in Fig. 5. The 20 nt long sequences of the sgRNAs were changed via

Gibson assembly (ClonExpress MultiS One Step Cloning Kit, Vazyme) using primers indicated in Table S2. The obtained pMEV4-dCas9 plasmids were transformed into *M. maripaludis* S0001 via the PEG-mediated transformation procedure and puromycin resistance transformants were obtained and verified.

#### Construction of the inducible CRISPRi-Cas9 system based on TetR-*tetO* for inducible CRISPRi

To obtain an inducible CRISPRi-dCas9 system, the applicable inducible promoters were first designed and tested for their ability to respond to an inducer such as anhydrotetracycline (aTc). Six *tetO* fused promoters were designed as shown in Fig. 6A and S3A and fused upstream the mCherry reporter gene and TetR was expressed adjacently using a constitutive promoter P0383 and terminator Tmcr that were assayed previously [17, 46]. The *tetR* gene was fused downstream a constitutive promoter of *PhmvA* [46], adjacent to the P0383/P0667-*tetO*-mCherry as shown in Fig. 6A and S3A. The fluorescence intensities of these six designed TetR-*tetO* promoters were detected in the presence and absence of the inducer anhydrotetracycline (aTc). Various aTc concentrations were tested in exponentially grown cultures added into the logarithmic cultures, and after 0 h, 1 h and 4 h, the fluorescence intensities were measured using a Synergy H4 Hybrid Multi-Mode Microplate Reader (BioTek Instruments) as previously described [46] and compared to that preceding the addition. Fluorescence intensities were detected using the procedure described below.

To construct an inducible CRISPRi-dCas9 system, the aTc inducible P0383-*tetO3* promoter was selected to express the dCas9 in the CRISPRi-dCas9 plasmid. The P0383-*tetO3* promoter sequence was fused upstream dCas9 sequence using ClonExpress MultiS One Step Cloning Kit (Vazyme). The expression of dCas9 induced by the addition of aTc was detected by western-blot assay. To target different genes, sgRNAs targeting different regions of genes were changed similarly as described above using ClonExpress MultiS One Step Cloning Kit (Vazyme) using primers indicated in Table S2. All the obtained plasmids were verified by DNA sequencing before transformed into *M. maripaludis* S0001.

#### RT-qPCR assay

Total RNA was extracted from the midexponential cells as described previously [16, 17]. 500 ng Total RNA were digested and reverse transcribed using ReverTra Ace qPCR RT Master Mix with gDNA Remover (Toyobo) and random hexamers according to the supplier's instructions and used for qPCR amplification with the corresponding primers (Table S2). Amplifications were performed with a Mastercycler ep realplex2 (Eppendorf

AG, Hamburg, Germany). Calculation of relative gene expression: CT values of different genes were obtained according to quantitative PCR results. Then, using 16 S rRNA as a standard reference [58, 59], the transcription abundance of each gene was normalized to 16 S rRNA in the sample. The difference of gene expression in different strains or different treatment conditions was analyzed. All measurements were performed on triplicate samples and repeated at least three times.

#### PEG-mediated transformation and colony selection of *M. maripaludis*

The constructed pMEV4 plasmids were transformed into *M. maripaludis* through polyethylene glycol (PEG)-mediated transformation, following a previously established procedure [13]. Prior to transformation, stock solutions were prepared. A 50 × cysteine/DTT solution (2.5% cysteine-HCl, 50 mM DTT) was prepared in a small serum bottle and filter-sterilized using disposable 0.22 μm filters. Transformation buffer (TB) was prepared in a 100-ml beaker by combining the following components: 50 mM Tris Base, 0.35 M sucrose, 0.38 M NaCl, 0.00001% resazurin, and 1 mM MgCl<sub>2</sub>. The pH was adjusted to 7.5 using HCl. The TB solution was transferred to a 100-ml serum bottle, and resazurin and 1 ml of the 50 × cysteine/DTT solution were added to make a final volume of 50 ml. TB+PEG was created by adding 40% (wt/vol) PEG8000 to the TB mixture. The serum bottles were sealed with serum stoppers and pressurized with H<sub>2</sub>/CO<sub>2</sub> (80:20, vol/vol) at 137 kPa for 10 s. Prior to use, TB and TB+PEG were sterilized at 121 °C for 20 min.

During the transformation process, 5 ml of *M. maripaludis* strains were cultured in an anaerobic tube, followed by centrifugation at 3000×g for 10 min. The supernatant was removed, and the pellet was resuspended by adding 5 ml of TB using an air-free needle. In a mini anaerobic tube, 20 μL of the plasmid, 20 μL of ddH<sub>2</sub>O, and 750 μL of TB were combined and pressurized with N<sub>2</sub>/CO<sub>2</sub> at 137 kPa. Then, 380 μL of the mixture from the mini anaerobic tube and 250 μL of TB+PEG was added to the previously prepared anaerobic tube. The tube was incubated at 37 °C for 1 h. To remove excess PEG, 5 ml of McF medium was added to the tube and centrifuged. Finally, another 5 ml of McF medium was added, and the tube was incubated overnight at 37 °C.

#### Western blot assay

Western blotting was performed using a similar procedure as described previously [16, 17]. Mid-exponential strains of *M. maripaludis* were harvested by centrifugation, resuspended in lysis buffer [20 mM Tris-Base, 150 mM NaCl, 10% (v/v) glycerol, 0.1% (v/v) Triton X-100], followed by sonication for cell lysis. The cell debris was then removed at 10,000 g for 10 min at 4 °C, and protein

concentration in the supernatant was determined using a BCA protein assay kit (Thermo Scientific). Proteins in the supernatant were separated by SDS-PAGE and then transferred to nitrocellulose membranes for Western blot analysis. The analysis was performed using customized polyclonal rabbit antisera raised against the purified Mmp-aCPSF1 protein. The immune-active bands were visualized using the Amersham ECL Prime Western blot detection reagent (GE Healthcare) on Tanon-5200 multi chemiluminescence/ fluorescence imaging system. The intensities of the Western blot band intensities were quantified using ImageJ.

#### mCherry fluorescence intensity assay

Expression of the mCherry reporter gene in *M. maripaludis* strains was quantified as described previously [16–18]. Briefly, colonies were cultured to exponential phase and cell density (OD600) was measured. Cells from 1 mL of culture were collected at 4 °C by centrifugation at  $17,900 \times g$ . Then the cells were resuspended, lysed with 200  $\mu$ L of 20 mM PIPES [piperazine-N, N'-bis(2-ethanesulfonic acid)], and then shaken for 12 h at 30 °C and 220 rpm. The samples were withdrawn and centrifuged at 30 °C and  $17,900 \times g$ . Next, the fluorescence of the supernatant with appropriate volume was measured on a Synergy H4 hybrid multimode microplate reader (BioTek Instruments) with excitation and emission wavelengths of 575 and 610 nm, respectively. The fluorescence intensity of mCherry was defined as the ratio of detected fluorescence units (RFUs) divided by the optical density (OD600) and the sample volume.

#### Curing of the pMEV4-Cas9 plasmid for new rounds of genome editing

The Cas9 plasmid needs to be cured from the initial gene-edited strain before the second round of the CRISPR-based editing. To achieve this goal, a counterselection marker, *hpt*, which was inserted into pMEV4 to facilitate the curing. The *hpt* marker confers sensitivity to the base analog 8-azahypoxanthine in the parental strain of *M. maripaludis* S0001, which is a  $\Delta hpt$  mutant [13]. To achieve the plasmid curing, the transformants with puromycin resistance were subcultured for four or five generations in liquid medium without puromycin, and then the culture was plated onto a solid counterselection medium containing 8-azahypoxanthine to obtain the 8-azahypoxanthine resistant transformants. Cells exhibiting a 8-azahypoxanthine resistance and are incapable of growing in puromycin containing medium, lost the plasmid and can be employed for the next round of genome editing.

#### Swarming motility analysis of *M. maripaludis* strains on semi-solid medium

The swarming motility ability of the *earA* knock-out and knock-down strains of *M. maripaludis* (shown in Figure S5) were compared with that of the wild type using the similar procedure described previously [22]. Five microliters of overnight cell cultures of each strain (OD600 normalized to 0.6) were incubated into the solid plates containing 0.25% agar (w/v). Plates were incubated anaerobically in a canister under an atmosphere of  $N_2:CO_2$  (80:20) at 37 °C for 4 days.

#### Supplementary Information

The online version contains supplementary material available at <https://doi.org/10.1186/s12934-024-02492-0>.

Supplementary Material 1

#### Acknowledgements

The authors thank Prof. William B. Whitman at the University of Georgia providing *Methanococcus maripaludis* strains and plasmid pMEV4.

#### Author contributions

J.L., X.Z.D., and L.P.B. conceptualized the projects, designed experiments, and acquired funding. Q.D., Y.F.W., L.Y.Z., D.R.R., and J.G. designed and performed the plasmid construction, genetic transformation, mCherry measuring and RT-qPCR experiments. All authors analyzed and discussed the experimental results. J.L., and X.Z.D. wrote the manuscript and all of the authors approved the final manuscript.

#### Funding

This work was supported by the National Natural Science Foundation of China (Grant nos. 32393974 and 32270054) and the National Key Research and Development Program of China (Grant nos. 2020YFA0906800 and 2019YFA0905500).

#### Data availability

No datasets were generated or analysed during the current study.

#### Declarations

#### Ethics approval and consent to participate

Not applicable.

#### Consent for publication

Yes.

#### Competing interests

The authors declare no competing interests.

#### Author details

<sup>1</sup>State Key Laboratory of Microbial Resources, Institute of Microbiology, Chinese Academy of Sciences, No.1 Beichen West Road, Beijing 100101, China

<sup>2</sup>University of Chinese Academy of Sciences, No.19A Yuquan Road, Shijingshan District, Beijing 100049, China

<sup>3</sup>Key Laboratory of Development and Application of Rural Renewable Energy, Biogas Institute of Ministry of Agriculture and Rural Affairs, Chengdu 610041, China

<sup>4</sup>Laboratory of Synthetic Microbiology, School of Chemical Engineering & Technology, Tianjin University, Tianjin 300072, China

<sup>5</sup>School of Basic Medical Sciences, School of Biomedical Engineering, Hubei University of Medicine, Shiyan, China

Published online: 04 September 2024

## References

- Spang A, Caceres EF, Ettema TJG. Genomic exploration of the diversity, ecology, and evolution of the archaeal domain of life. *Science*. 2017;357(6351).
- Castelle CJ, Banfield JF. Major New Microbial Groups Expand Diversity and alter our understanding of the Tree of Life. *Cell*. 2018;172(6):1181–97.
- Pace NR. A molecular view of microbial diversity and the biosphere. *Science*. 1997;276(5313):734–40.
- Li J et al. The archaeal transcription termination factor aCPSF1 is a robust phylogenetic marker for archaeal taxonomy. *Microbiol Spectr*. 2021;9(3).
- Baker BJ, et al. Diversity, ecology and evolution of Archaea. *Nat Microbiol*. 2020;5(7):887–900.
- Pfeifer K, et al. Archaea Biotechnol *Biotechnol Adv*. 2021;47:107668.
- Li J et al. *Archaea in Wastewater Treatment: Current Research and Emerging Technology* Archaea-an International Microbiological Journal, 2018. 2018: 6973294.
- Rodrigo-Banos M, et al. Carotenoids from Haloarchaea and their potential in Biotechnology. *Mar Drugs*. 2015;13(9):5508–32.
- Mauerhofer LM, et al. Hyperthermophilic methanogenic archaea act as high-pressure CH<sub>4</sub> cell factories. *Commun Biology*. 2021;4(1):289.
- Kershanthen Thevasundaram JGG, Freeman Cherng, Michelle CY, Chang. Engineering nonphotosynthetic carbon fixation for production of bioplastics by methanogenic archaea. *Proc Natl Acad Sci USA*. 2022;119(23):e2118638119.
- Goyal N, Zhou Z, Karimi IA. Metabolic processes of Methanococcus maripaludis and potential applications. *Microb Cell Fact*. 2016;15:107.
- Li J, Shao TSAN, Chen C, Dong X, Liu Y, Whitman WB. Genetic and metabolic engineering of Methanococcus spp. *Curr Res Biotechnol*, 2023. 5.
- Sarmiento BF, Leigh JA, Whitman WB. *Genetic Systems for Hydrogenotrophic Methanogens* Methods in Enzymology: Methods in Methane Metabolism, Pt A, 2011. 494: pp. 43–73.
- Lyu Z, Whitman WB. Transplanting the pathway engineering toolbox to methanogens. *Curr Opin Biotechnol*. 2019;59:46–54.
- Lyu Z, et al. Engineering the Autotroph Methanococcus maripaludis for Geraniol Production. *ACS Synth Biol*. 2016;5(7):577–81.
- Yue L, et al. The conserved ribonuclease aCPSF1 triggers genome-wide transcription termination of Archaea via a 3'-end cleavage mode. *Nucleic Acids Res*. 2020;48(17):9589–605.
- Li J, et al. aCPSF1 cooperates with terminator U-tract to dictate archaeal transcription termination efficacy. *Elife*. 2021;10:e70464.
- Li J, et al. The archaeal RNA chaperone TRAM0076 shapes the transcriptome and optimizes the growth of Methanococcus maripaludis. *PLoS Genet*. 2019;15(8):e1008328.
- Zhang W, et al. Internal transcription termination widely regulates differential expression of operon-organized genes including ribosomal protein and RNA polymerase genes in an archaeon. *Nucleic Acids Res*. 2023;51(15):7851–67.
- Qi L, et al. Endonucleolytic processing plays a critical role in the maturation of ribosomal RNA in Methanococcus maripaludis. *RNA Biol*. 2023;20(1):760–73.
- Ding Y, et al. Identification of the first transcriptional activator of an archaeal lum operon in a euryarchaeon. *Mol Microbiol*. 2016;102(1):54–70.
- Ding Y, et al. Bypassing the need for the transcriptional activator EarA through a spontaneous deletion in the BRE portion of the fla operon promoter in Methanococcus maripaludis. *Front Microbiol*. 2017;8:1329.
- Kessler PS, Leigh JA. Genetics of nitrogen regulation in Methanococcus maripaludis. *Genetics*. 1999;152(4):1343–51.
- Cohen-Kupiec R, Blank C, Leigh JA. Transcriptional regulation in Archaea: in vivo demonstration of a repressor binding site in a methanogen. *Proc Natl Acad Sci U S A*. 1997;94(4):1316–20.
- Dodsworth JA, Leigh JA. Regulation of nitrogenase by 2-oxoglutarate-reversible, direct binding of a PII-like nitrogen sensor protein to dinitrogenase. *Proc Natl Acad Sci USA*. 2006;103(26):9779–84.
- Lie TJ, Wood GE, Leigh JA. Regulation of nif expression in Methanococcus maripaludis: roles of the euryarchaeal repressor NrpR, 2-oxoglutarate, and two operators. *J Biol Chem*. 2005;280(7):5236–41.
- Costa KC, et al. Effects of H<sub>2</sub> and formate on growth yield and regulation of methanogenesis in Methanococcus maripaludis. *J Bacteriol*. 2013;195(7):1456–62.
- Shalvarjian KE, Nayak DD. Transcriptional regulation of methanogenic metabolism in archaea. *Curr Opin Microbiol*. 2021;60:8–15.
- Goyal N, et al. A genome-scale metabolic model of Methanococcus maripaludis S2 for CO<sub>2</sub> capture and conversion to methane. *Mol Biosyst*. 2014;10(5):1043–54.
- Lupa B, et al. Formate-dependent H<sub>2</sub> production by the mesophilic methanogen Methanococcus maripaludis. *Appl Environ Microbiol*. 2008;74(21):6584–90.
- Li J, et al. CRISPR-Cas9 Toolkit for Genome Editing in an autotrophic CO<sub>2</sub>-Fixing Methanogenic Archaeon. *Microbiol Spectr*. 2022;10(4):e0116522.
- Bao J. Silvan Scheller *Efficient CRISPR/Cas12a-Based genome-editing toolbox for Metabolic Engineering in Methanococcus maripaludis*. *ACS Synth Biol*. 2022;11(7):2496–503.
- Koonin EV, Makarova KS, Zhang F. Diversity, classification and evolution of CRISPR-Cas systems. *Curr Opin Microbiol*. 2017;37:67–78.
- Makarova KS, et al. Evolutionary classification of CRISPR-Cas systems: a burst of class 2 and derived variants. *Nat Rev Microbiol*. 2020;18(2):67–83.
- Pickar-Oliver A, Gersbach CA. The next generation of CRISPR-Cas technologies and applications. *Nat Rev Mol Cell Biol*. 2019;20(8):490–507.
- Komor AC, Badran AH, Liu DR. CRISPR-Based technologies for the manipulation of eukaryotic genomes. *Cell*. 2017;169(3):559.
- Barrangou R, van Pijkeren JP. Exploiting CRISPR-Cas immune systems for genome editing in bacteria. *Curr Opin Biotechnol*. 2016;37:61–8.
- Lei S, Qi MHL, Luke A, Gilbert JA, Doudna JS, Weissman AP, Arkin, Wendell A, Lim. Repurposing CRISPR as an RNA-guided platform for sequence-specific control of gene expression. *Cell*. 2013;152(5):1173–83.
- Choudhary E, et al. Gene silencing by CRISPR interference in mycobacteria. *Nat Commun*. 2015;6:6267.
- Yao L, et al. Multiple gene repression in Cyanobacteria using CRISPRi. *ACS Synth Biol*. 2016;5(3):207–12.
- Kim SK, et al. CRISPR interference-mediated gene regulation in Pseudomonas putida KT2440. *Microb Biotechnol*. 2020;13(1):210–21.
- Benjamin M, Woolston DFE, Devin H, Currie G, Stephanopoulos. Redirecting carbon flux in Clostridium ljungdahlii using CRISPR interference (CRISPRi). *Metab Eng*. 2018;48:243–53.
- Dhamad AE, Lessner DJ. A CRISPRi-dCas9 system for Archaea and its Use to examine gene function during Nitrogen fixation by Methanosarcina acetivorans. *Appl Environ Microbiol*, 2020. 86(21).
- Qi L, et al. Genome-wide mRNA processing in methanogenic archaea reveals post-transcriptional regulation of ribosomal protein synthesis. *Nucleic Acids Res*. 2017;45(12):7285–98.
- Hildenbrand C, et al. Genome copy numbers and gene conversion in methanogenic archaea. *J Bacteriol*. 2011;193(3):734–43.
- Xu Q, et al. A robust genetic toolbox for fine-tuning gene expression in the CO<sub>2</sub>-Fixing methanogenic archaeon Methanococcus maripaludis. *Metab Eng*. 2023;79:130–45.
- Sarmiento F, Mrazek J, Whitman WB. Genome-scale analysis of gene function in the hydrogenotrophic methanogenic archaeon Methanococcus maripaludis. *Proc Natl Acad Sci U S A*. 2013;110(12):4726–31.
- Qi L, et al. Comprehensive analysis of the pre-ribosomal RNA maturation pathway in a methanoarchaeon exposes the conserved circularization and linearization mode in archaea. *RNA Biol*. 2020;17(10):1427–41.
- Thomas Veith RM, Jan P, Wurm BL, Weis E, Duchardt-Ferner C, Saffertal R, Hennig O, Mirus, Markus T, Bohnsack, Jens Wöhnert, Enrico Schleiff, *Structural and functional analysis of the archaeal endoribonuclease Nob1*. *Nucleic Acids Res*. 2012;40(7):3259–74.
- Kabin Xie BM, Yang Y. Boosting CRISPR/Cas9 multiplex editing capability with the endogenous tRNA-processing system. *Proc Natl Acad Sci U S A*. 2015;112(11):3570–5.
- Aris-Edda Stachler TSS, Schreiber S, Marchfelder A. CRISPRi as an efficient tool for gene repression in archaea. *Methods*. 2020;172:76–85.
- Akinyemi TS, et al. Tuning Gene expression by phosphate in the Methanogenic Archaeon Methanococcus maripaludis. *ACS Synth Biol*. 2021;10(11):3028–39.
- Stachler AE, Marchfelder A. Gene repression in Haloarchaea using the CRISPR (clustered regularly interspaced short palindromic Repeats)-Cas I-B system. *J Biol Chem*. 2016;291(29):15226–42.
- Moore BC, Leigh JA. Markerless mutagenesis in Methanococcus maripaludis demonstrates roles for alanine dehydrogenase, alanine racemase, and alanine permease. *J Bacteriol*. 2005;187(3):972–9.
- Doudna JA, Charpentier E. The new frontier of genome engineering with CRISPR-Cas9. *Science*. 2014;346(6213):1077–.

56. Walters AD, Smith SE, Chong JP. Shuttle vector system for *Methanococcus maripaludis* with improved transformation efficiency. *Appl Environ Microbiol*. 2011;77(7):2549–51.
57. Tumbula DL, Makula RA, Whitman WB. Transformation of *Methanococcus Maripaludis* and Identification of a PstI-Like Restriction System. *FEMS Microbiol Lett*. 1994;121(3):309–14.
58. Xia QW, et al. Quantitative proteomics of the archaeon validated by microarray analysis and real time PCR. *Cell Proteom*. 2006;5(5):868–81. Molecular.
59. Rother M, Sattler C, Stock T. *Studying Gene Regulation in Methanogenic Archaea* Methods in Enzymology: Methods in Methane Metabolism, Pt A, 2011. 494: pp. 91–110.

### **Publisher's Note**

Springer Nature remains neutral with regard to jurisdictional claims in published maps and institutional affiliations.